Available online at www.sciencedirect.com
ScienceDirect
Catalysis Today 126 (2007) 387–393
CATALYSIS TODAY
www.elsevier.com/locate/cattod

Decolorization of reactive brilliant red X-3B by heterogeneous photo-Fenton reaction using an Fe–Ce bimetal catalyst

Yu Zhang [a,b], Xiaomin Dou [a,c], Jian Liu [a,c], Min Yang [a,*], Liping Zhang [a,c], Yoichi Kamagata [b,d]

[a] State Key Laboratory of Environmental Aquatic Chemistry, Research Center for Eco-Environmental Sciences, Chinese Academy of Sciences, P.O. Box 2871, Beijing 100085, China
[b] Institute for Biological Resources and Functions, National Institute of Advanced Industrial Science and Technology, Tsukuba, Ibaraki 305-8566, Japan
[c] Beijing Forestry University, Beijing 100083, China
[d] Research Institute of Genome-based Biofactory, National Institute of Advanced Industrial Science and Technology, Sapporo 062-8517, Japan

Available online 19 July 2007

Abstract

Decolorization of reactive brilliant red X-3B was studied by using an Fe–Ce oxide hydrate as the heterogeneous catalyst in the presence of H_2O_2 and UV. The decolorization rate was in the order of UV–Fe–Ce–H_2O_2 > UV–Fe^{3+}–H_2O_2 > UV–H_2O_2 > UV–Fe–Ce ≥ Fe–Ce–H_2O_2 > Fe–Ce. Under the conditions of 34 mg l^{-1} H_2O_2, 0.500 g l^{-1} Fe–Ce, 36 W UV and pH 3.0, 100 mg l^{-1} X-3B could be decolorized at efficiency of more than 99% within 30 min. The maximum dissolved Fe during the reaction was 1 mg l^{-1}. From the fact that the decolorization rate of the UV–Fe–Ce–H_2O_2 system was significantly higher than that of the UV–Fe^{3+}–H_2O_2 system at Fe^{3+} = 1 mg l^{-1}, it is clear that the Fe–Ce functioned mainly as an efficient heterogeneous catalyst. UV–vis, its second derivative spectra, and ion chromatography (IC) were employed to investigate the degradation pathway. Fast degradation after adsorption of X-3B is the dominant mechanism in the heterogeneous catalytic oxidation system. The first degradation step is the breaking down of azo and C–N bonds, resulting in the formation of the aniline- and phenol-like compounds. Then, the breaking down of the triazine structure occurred together with the transformation of naphthalene rings to multi-substituted benzene, and the cutting off of sulphonic groups from the naphthalene rings. The last step includes further decomposition of the aniline structure and partial mineralization of X-3B.

Keywords: Reactive brilliant red X-3B; Fe–Ce catalyst; Photo-Fenton reaction; Heterogeneous catalysis; Decolorization; Mechanism

1. Introduction

The homogeneous photo-Fenton process has attracted wide interest because of its relatively low cost and high performance in generating OH radicals for the decomposition of refractory organic compounds [1–5]. This process, however, produces a lot of sludge during treatment, which limits its wide application in wastewater treatment. To overcome this disadvantage of the homogeneous photo-Fenton process, efforts have been devoted to preparing heterogeneous iron catalysts by coating Fe ions or Fe oxide onto porous solid supporting materials [5–8].

A good heterogeneous iron catalyst should meet two requirements: it must have high catalytic activity and low Fe dissolution. The α-FeOOH based heterogeneous catalyst has demonstrated high treatment efficiency in photooxidation of azo dye [9]. The dissolved Fe concentration, however, was as high 0.5 g l^{-1}, which is not acceptable for application. Fernandez et al. [10] have succeeded in the preparation of an Fe^{3+}–Nafion catalyst for the photo-assisted degradation of Orange II. However, it should be stressed that the Nafion film-based catalyst is too expensive to be used for practical application even though the catalyst can be separated easily from the solution.

In our previous studies, Ce doped Fe oxide materials were developed for the removal of hazardous anions and natural organic substance from groundwater [11]. The Fe–Ce bimetal oxide hydrate has a solid solution structure, which is characterized by a high concentration of surface hydroxyl groups (M–OH) [12]. It is assumed that such a solid solution structure might be useful for photocatalysis. And further, it has been reported that cerium ion has a role as an assistant in photocatalysis [13]. So, in this study the Fe–Ce bimetal oxide

* Corresponding author. Tel.: +86 10 62923475; fax: +86 10 62923541.
E-mail addresses: yangmin@rcees.ac.cn, zhangyu@rcees.ac.cn (M. Yang).

0920-5861/$ – see front matter © 2007 Elsevier B.V. All rights reserved.
doi:10.1016/j.cattod.2007.06.019

hydrate was used as a heterogeneous catalyst for the degradation of a common textile dye (X-3B) in the presence of H_2O_2 and UV light. This dye has high solubility in water (80 g l^{-1}) and is red in color. In China, more than 1.6×10^9 m^3 per year of various dye wastewater is drained into rivers without satisfactory treatment, and depollution is the first concern. The effects of initial X-3B concentration, H_2O_2 concentration, UV light wavelength and power, and Fe–Ce catalyst loading, on the decolorization of X-3B have been documented [14]. The present study compared the efficiency of the UV–Fe–Ce–H_2O_2 system for the decolorization of X-3B with some related systems. The dye degradation pathway was also proposed based on the results from UV–vis spectra, its second derivative spectra, and ion chromatography (IC).

2. Materials and methods

2.1. Materials

Reactive brilliant red X-3B (X-3B) (Tianjin Tianshun Chemical Company, China) was used without further purification. Fig. 1 shows the chemical structure of X-3B. All other chemical reagents were analytical grade. The Fe–Ce oxide hydrate catalyst was prepared by the coprecipitation method [11] and its surface properties have been reported in detail [12]. 0.08 mol l^{-1} $Ce(SO_4)_2{\cdot}4H_2O$ was dissolved in 2 l of distilled water together with 0.2 mol l^{-1} $FeCl_3{\cdot}6H_2O$ and 0.1 mol l^{-1} $FeCl_2{\cdot}4H_2O$. Under gentle stirring, the pH was slowly raised to around 10 by the addition of 6 mol l^{-1} NaOH solution. Stirring was further continued for 30 min to maintain the pH at 10. After 10 h of aging at room temperature, the suspension was repeatedly washed with distilled water and then was dried at 100 °C for 10 h. The dry material was ground and stored in a desiccator.

2.2. Photoreactor

A laboratory-scale batch photoreactor was employed as shown in Fig. 2. The photoreactor used was cylindrical with one UV lamp (36-W, $\lambda = 254$ nm) inside a quartzose tube. The available volume of the reactor was 1500 ml. In order to effectively suspend the Fe–Ce catalyst in the reactor and ensure good mixing, compressed air was bubbled from the bottom to the top of the reactor. The total volume of the solution was 1000 ml, and the initial solution pH was controlled at 3.0. The starting point of the reaction was defined as the time when a certain amount of H_2O_2 was added to the photoreactor and the UV light was turned on. At certain reaction intervals, 5-ml samples were withdrawn and filtrated with 0.45 μm membrane filter for analysis. The experimental setup was wrapped with aluminium foil. Experiments were repeated three times, and all of the data are the average of the three.

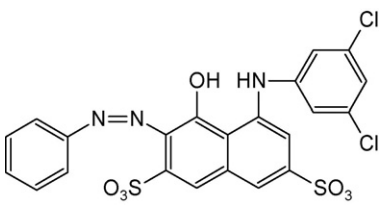

Fig. 1. Chemical structure for reactive brilliant red X-3B.

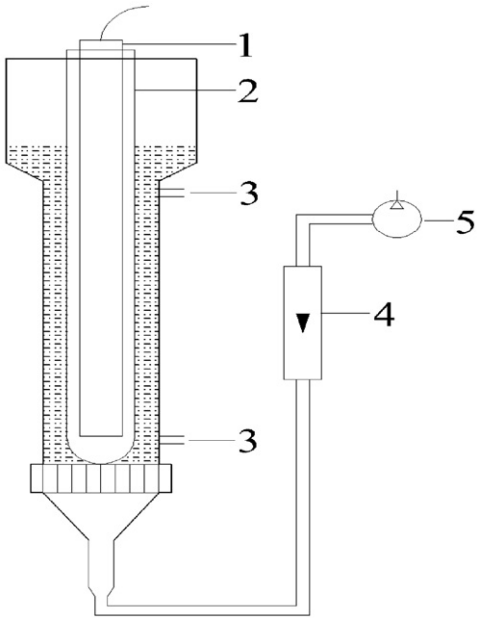

Fig. 2. Experimental setup used in this study: (1) UV lamp, (2) quartzose tube, (3) sampling pipe, (4) flowmeter and (5) compressed air.

The initial concentration of each of the desired components was kept the same for all the experiments performed in this study, which was $[X\text{-}3B]_0 = 100$ mg l^{-1}, $[H_2O_2]_0 = 34$ mg l^{-1}, Fe–Ce at 0.500 g l^{-1}, and Fe^{3+} at 1.0 mg l^{-1} according to the optimal conditions reported in our previous work [14].

2.3. Analysis

The concentration of X-3B in water was determined by the absorption intensity at 540 nm using a UV–vis spectrometer (Hitachi UV U-3100, Japan). Changes in the concentration of H_2O_2 were monitored with titanium tetrachloride colorimetry. Ionic chromatography (Dionex Series 4500i, USA) was used to detect the concentrations of SO_4^{2-} and Cl^- in the photodegradaton of X-3B.

3. Results and discussion

3.1. Decolorization of X-3B in different systems

The decolorization performance of X-3B in different systems is compared in Fig. 3. The dye X-3B in water has four strong absorption bands (234, 280, 330, and 540 nm), corresponding to the structures of benzene, triazine, naphthalene, and a conjugated system linked by two azo groups, respectively (Figs. 1 and 5 (0 min)). As shown in Fig. 3, these structures are quite stable to UV irradiation or the introduction of H_2O_2 alone. Decolorization of X-3B was observed in the dark system containing 0.500 g l^{-1} Fe–Ce. The removal of dye in this case, however, was attributed to the adsorption by the

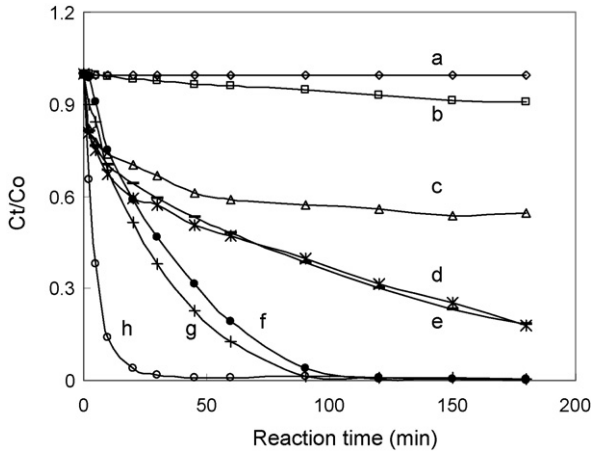

Fig. 3. Decolorization of the dye X-3B (100 mg l^{-1}) in water under different conditions: (a) with 34 mg l^{-1} H_2O_2; (b) under 36 W UV irradiation; (c) with 0.500 g Fe–Ce l^{-1}; (d) with 0.500 g Fe–Ce l^{-1} and 34 mg l^{-1} H_2O_2; (e) with 0.500 g Fe–Ce l^{-1} and 36 W UV; (f) with 34 mg l^{-1} H_2O_2 and 36 W UV; (g) with 34 mg l^{-1} H_2O_2, 1 mg l^{-1} Fe^{3+}, and 36 W UV; (h) with 34 mg l^{-1} H_2O_2, 0.500 g Fe–Ce l^{-1}, and 36 W UV.

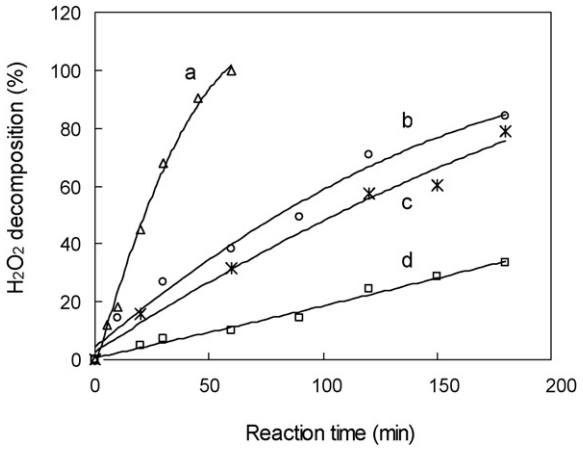

Fig. 4. Decomposition of H_2O_2 under different conditions: (a) with 34 mg l^{-1} H_2O_2, 0.500 g Fe–Ce l^{-1}, and 36 W UV; (b) with 34 mg l^{-1} H_2O_2, 1 mg l^{-1} Fe^{3+}, and 36 W UV; (c) without Fe–Ce but with 34 mg l^{-1} H_2O_2 and 36 W UV; (d) with 34 mg l^{-1} H_2O_2 and 0.500 g Fe–Ce l^{-1}.

catalyst. With the addition of H_2O_2 or UV irradiation, the decolorization rates of the Fe–Ce system increased significantly. However the decolorization rates were markedly lower than that of the UV–H_2O_2 system. The heterogenous photo-Fenton system demonstrated the best decolorization efficiency, and the relative dye degradation efficiency of each oxidation system can be ranked in the order of UV–Fe–Ce–H_2O_2 > UV–Fe^{3+}–H_2O_2 > UV–H_2O_2 > UV–Fe–Ce ≥ Fe–Ce–H_2O_2 > UV.

In the UV–Fe–Ce–H_2O_2 system, dissolution of Fe from the catalyst was observed [14]. The dissolved total Fe concentration increased with the elapse of time, and the maximum concentration was 1 mg l^{-1}, which was identical to that in the homogeneous system in Fig. 3. This demonstrates that Fe ion leaching from the Fe–Ce catalyst was very low in comparison with leaching from other heterogeneous catalysts [5,9]. The Fe leaching was observed not only in the UV–Fe–Ce–H_2O_2 system, but also in other systems containing the Fe–Ce material. However, the maximum concentrations of the total dissolved Fe in other systems were less than 1 mg l^{-1}. In our previous study, XPS spectra demonstrated that the dominating chemical state of Fe was Fe(III) in Fe–Ce catalyst [12]. Recently, a reasonable hypothesis of complex and leaching of Fe(II) from Fe(III) containing catalysts as a result of photochemical reduction of Fe(III) species has been proposed [15]. Fe^{2+} leached out in the aqueous phase was possibly reoxidized to Fe^{3+} by H_2O_2. Fe^{3+} might therefore be the dominating species in the aqueous phase.

On the other hand, the UV–Fe–Ce–H_2O_2 system demonstrated much better decolorization performance than that of the homogenous photo-Fenton system constituted by adding 1 mg l^{-1} Fe^{3+} in the solution (Fig. 3(g)). And by comparing the homogenous photo-Fenton system with that of UV–H_2O_2, it is clear that the decolorization contribution by the homogenous photo-Fenton system at an Fe^{3+} concentration of 1 mg l^{-1} was very small, and can be neglected. So, it can be concluded that heterogeneous catalysis played a key role in the decolorization of X-3B by the UV–Fe–Ce–H_2O_2 system.

3.2. Decomposition of H_2O_2 in different systems

In an advanced oxidation process (AOP) system using H_2O_2 as the oxidant, it is assumed that the production rate of OH radicals is in proportion to the decomposition rate of H_2O_2 [5]. The H_2O_2 decomposition rates of four systems were compared in Fig. 4. It is clear that the H_2O_2 decomposition rate of the UV–Fe–Ce–H_2O_2 system was much higher than the other three systems: UV–Fe^{3+}–H_2O_2, UV–H_2O_2, and Fe–Ce–H_2O_2, suggesting that the UV–Fe–Ce–H_2O_2 system was the most efficient system for producing OH radicals.

Fig. 4 also shows that H_2O_2 was completely decomposed in 60 min in the heterogeneous photo-Fenton reaction. A reasonable reaction mechanism for the generation of OH radicals has been given by Martínez et al. [15]. The photocatalytic decomposition of H_2O_2 leads to the generation of OH radicals during the dye degradation process. So in the first 60 min, the OH radicals derived from photocatalytic decomposition should have played an important role in the dye degradation.

3.3. Decolorization mechanisms

3.3.1. UV–vis absorption spectra of different systems

To investigate the decolorization mechanisms of X-3B, variations of the UV–vis absorption spectra of X-3B solution in each system were followed (Fig. 5). In the Fe–Ce system (Fig. 5(a)), the four main absorption bands of X-3B decreased at the same time without changing their shapes even after 180 min, which further verified the assumption that the decolorization was only caused by adsorption to the Fe–Ce catalyst in this system. Fig. 5(b) and (c) shows that the absorption bands at 330 and 280 nm disappeared after 60 min in the UV–Fe–Ce or H_2O_2–Fe–Ce system, showing that slow decomposition of some parts of the dye molecule occurred together with adsorption. Fig. 5(c) also indicates that the UV–Fe–Ce system should be the dominating source of OH radicals after the depletion of H_2O_2 (after 60 min), and might have played the key role for the decomposition of the dye

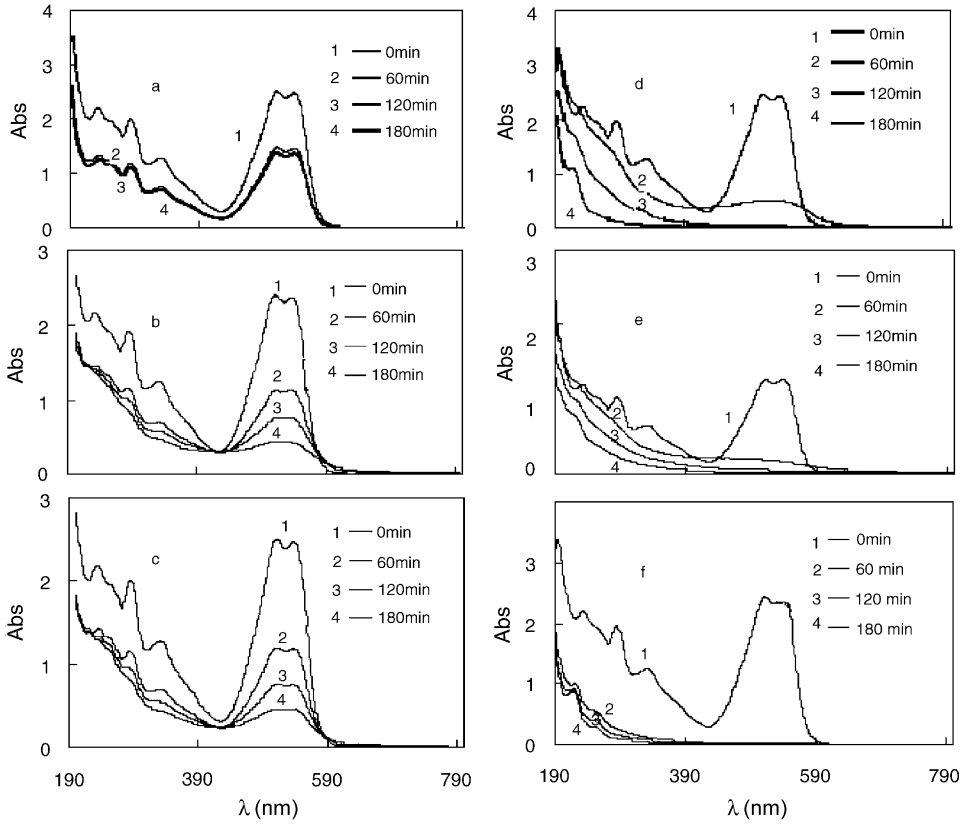

Fig. 5. UV–vis spectra changes of X-3B before and after different processes: (a) with 0.500 g Fe–Ce l^{-1}; (b) with 0.500 g Fe–Ce l^{-1} and 34 mg l^{-1} H_2O_2; (c) with 0.500 g Fe–Ce l^{-1} and 36 W UV; (d) with 34 mg l^{-1} H_2O_2 and 36 W UV; (e) with 34 mg l^{-1} H_2O_2, 1 mg l^{-1} Fe^{3+}, and 36 W UV; (f) with 34 mg l^{-1} H_2O_2, 0.500 g Fe–Ce l^{-1}, and 36 W UV.

decomposition intermediates. Fig. 5(d)–(f) shows that fast decomposition of the dye appeared in the UV–Fe–Ce–H_2O_2, UV–Fe^{3+}–H_2O_2, and UV–H_2O_2 systems, since all of the peaks except for that at 234 nm almost disappeared within 120 min.

3.3.2. *Degradation pathway of UV–Fe–Ce–H_2O_2 system*

As mentioned in Section 2.1, the dye X-3B has four structure units: benzene, triazine, naphthalene rings, and a conjugated system linked by two azo groups. In the UV region, the absorbance bands at 234, 280, and 330 nm are attributed to the benzene ring, triazine ring, and naphthalene ring, respectively, whereas the visible band at 540 nm is designated to the long conjugated π system linked by two azo groups [16,17]. In this section, we examined the changes of the second derivative spectra of dye solutions during the heterogeneous photo-Fenton reaction for better understanding the dye degradation pathway.

Changes of the UV–vis and its second derivative spectra of X-3B with time in the heterogeneous photo-Fenton system are respectively shown in Fig. 6. Five minutes after the start of the reaction, the strength of each band decreased, with its original shape remaining. It was speculated that the dominant process in the first 5 min was the adsorption of dye by the Fe–Ce catalyst.

After 10 min reaction, however, the band at 540 nm disappeared, and the bands at 330 and 280 nm became very weak, indicating that the azo groups and C–N single bonds conjoining the naphthalene and triazine rings were broken (Fig. 6(c-right)). At the same time, two new bands at 203 and 211 nm appeared. These new bands correspond to aniline cations and phenol-like structures, respectively [18]. It has been reported that the oxidation of azo bonds by OH radicals in the azo dyes led to decolorization of dye solutions with the formation of primary aromatic amines [19]. The formation of anilines suggested that the reductive cleavage of azo bonds occurred prior to the breaking of aromatic rings [20]. The formation of aromatic amines has also been reported in the natural anaerobic degradation of azo dyes [21]. Since the ring with amino groups is the first target of the hydroxyl radicals [22], the aniline molecules released from the breaking of azo bonds were possibly attacked by OH radicals and converted to phenols. The formation of phenolic compounds as intermediates is commonly observed in the photocatalytic degradation of other aromatic compounds or azo dyes [23,24]. The dye molecule was broken within 10 min, and some aniline-like and phenol-like molecules were formed.

Following 60 min oxidation, the original absorption bands attributed to triazine and naphthalene rings (at 280 and 330 nm) disappeared (Fig. 6(d-right)). At the same time, another new band at 258 nm (Fig. 6(d-left)), corresponding to multi-substituted benzene produced from degradation of the naphthalene ring [16,25], appeared. The triazine ring at 280 nm could be converted to cyanuric acid (OOOT), which was very stable in photocatalysis [26,27]. The band at 234 nm related to the benzene ring in the second derivative spectra still

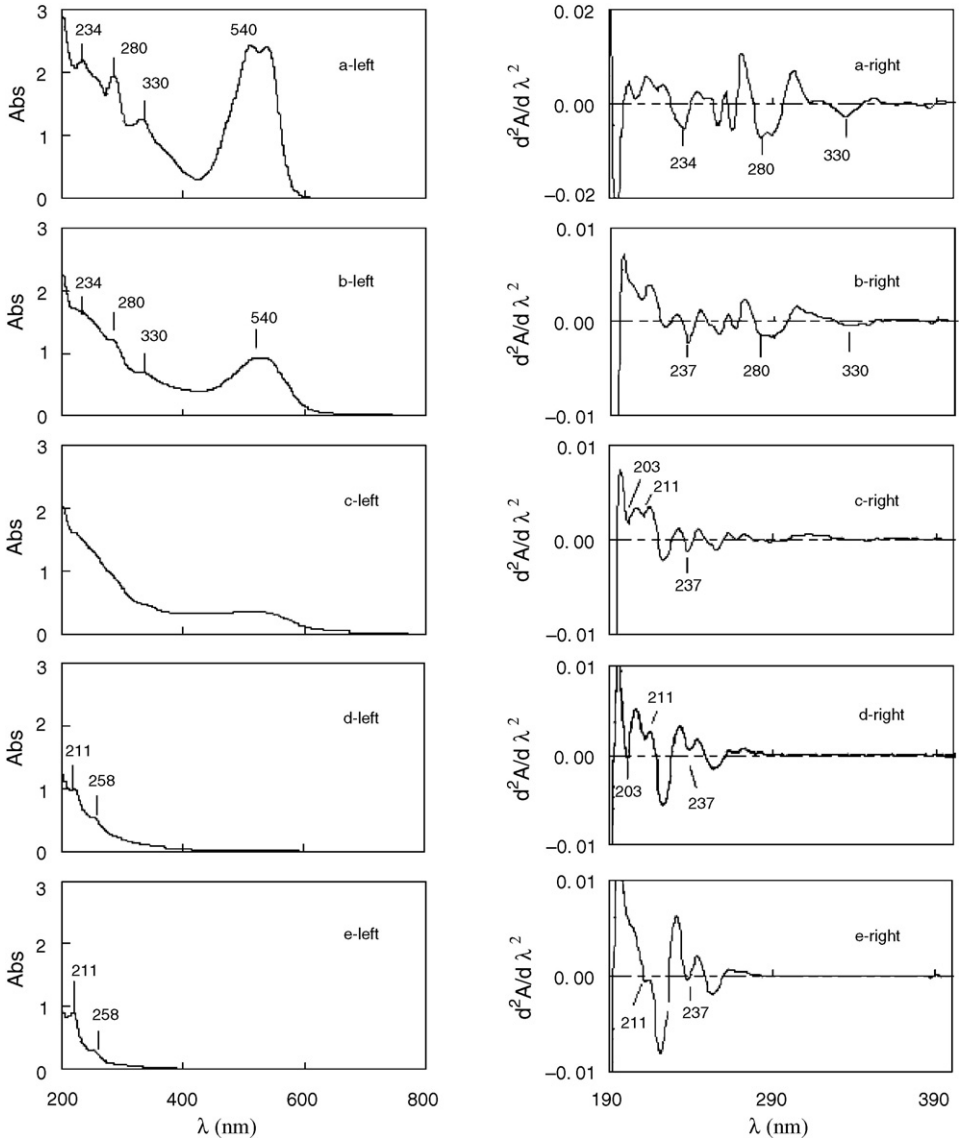

Fig. 6. UV–vis and its second derivative spectra changes of X-3B of heterogeneous photo-Fenton reaction using Fe–Ce catalyst: (a) 0 min; (b) 5 min; (c) 10 min; (d) 60 min; (e) 180 min.

existed although no color remained in the solution. Since naphthalene ring also could be degraded to aniline molecules, the band at 203 nm became much stronger at 60 min and then disappeared at 180 min (Fig. 6(d) and (e-right)).

In order to obtain more information about the degradation of the dye, the sulphate and chloride ions during the reaction were followed (Fig. 7). Although decolorization was completed in the first 30 min, almost no sulphate was detected. After oxidation for 60 min, however, high concentrations of sulphate appeared. So, sulphonic groups began to be broken off from the naphthalene ring after oxidation for more than 30 min. On the other hand, almost no chloride ions were detected during the whole experiment, indicating that the C–Cl bond could resist photocatalysis.

Therefore, in 10–60 min, the triazine ring was destructed, and the naphthalene ring was transformed to multi-substituted benzene. The cutting off of sulphonic groups from the naphthalene rings was one of the main reactions in the second

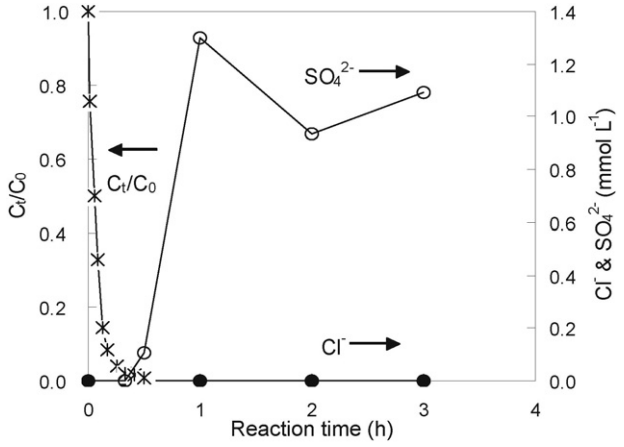

Fig. 7. Changes of SO_4^{2-} and Cl^- concentration during the photocatalytic degradation of X-3B.

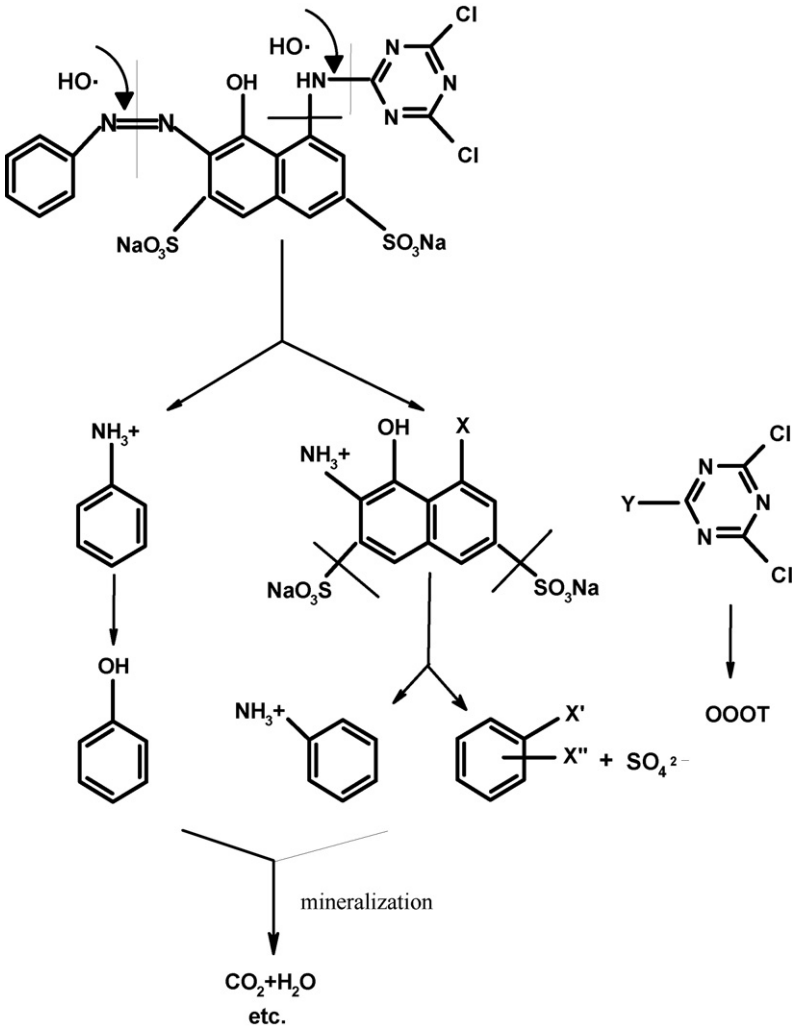

Fig. 8. Simplified degradation pathway of X-3B by heterogeneous photo-Fenton reaction using Fe–Ce catalyst.

step. However, it is very difficult to cut chlorine from the chlorinated benzene and triazene rings.

In the last degradation step at 180 min (Fig. 6(e-right)), the band at 203 nm disappeared, indicating that aniline might be decomposed.

Fig. 8 schematically presents the simplified degradation pathway of dye X-3B with heterogeneous photo-Fenton reaction using the Fe–Ce catalyst. The first step is the breaking down of azo and C–N bonds after adsorption. Aniline-like and phenol-like compounds were formed during this step. Triazene was degraded, and the naphthalene ring was transformed to multi-substituted benzene. At the same time, sulphonic groups began to be cut off from the naphthalene rings, accompanied with the formation of sulphate ions. The aniline-like compounds could be oxidized further. However, the chlorinated benzene and triazene rings were very stable during the oxidation.

The above results clearly reveal that the degradation reaction proceeds stepwise. Firstly, complete decolorization of 100 mg l^{-1} X-3B can be almost achieved in 30 min in the presence of 1.0 g Fe–Ce catalyst, 34 mg l^{-1} H_2O_2 and 36 W UV, indicating that decolorization of X-3B is a fast process. Previous studies [5,28] indicated that OH radicals can react with most organic compounds by hydrogen abstraction or addition to double bonds. Thus, in the case of X-3B, OH radicals first attack azo groups and open the N=N bonds, destructing the long conjugated π systems, and consequently causing decolorization. Since aromatic ring structures are more difficult to be destructed than the N=N bonds, the elimination of adjacent ring structures needs a longer time.

4. Conclusions

An Fe–Ce bimetal heterogeneous catalyst was used for X-3B removal by heterogeneous photo-Fenton reaction. The UV–Fe–Ce–H_2O_2 system demonstrated much better decolorization performance than all of the other related systems. The Fe–Ce catalyst showed a high H_2O_2 decomposition rate with low Fe dissolution. The heterogeneous photocatalysis, rather than the homogeneous one, played a key role in the decolorization of X-3B.

The first oxidation step is the breaking down of azo and C–N bonds by OH radicals with the formation of aniline-like and phenol-like compounds. Triazene was degraded, and the naphthalene rings were transformed to multi-substituted

benzene. At the same time, sulphonic groups began to be cut off from the naphthalene rings, accompanied with the formation of sulphate ions. Further studies using LC–MS and other techniques, however, are required to confirm the above speculation.

Acknowledgments

This work was supported by 863 projects (2004AA649280; 2002AA601300) and the National Natural Science Foundation of China (20207013). The authors are thankful to Prof. Hong He, Prof. Yizhong Wang, and Dr. Aimin Wang of RCEES, CAS, for their kind help. The authors are also thankful to the Postdoctoral Fellowship for the Foreign Researcher by the Japan Society for the Promotion of Science (JSPS).

References

[1] J.J. Pignatello, Environ. Sci. Technol. 26 (1992) 944.
[2] G. Ruppert, R. Bauer, G. Heisler, Chemosphere 28 (1994) 1447.
[3] S.F. Kang, C.H. Liao, H.P. Hung, J. Hazard. Mater. B 65 (1999) 317.
[4] A. Safarzadeh-Amiri, J.R. Bolton, S.R. Cater, Water Res. 31 (1997) 787.
[5] J.Y. Feng, X.J. Hu, P.L. Yue, H.Y. Zhu, G.Q. Lu, Water Res. 37 (2003) 3776.
[6] J. Fernandez, J. Bandara, A. Lopez, P.H. Buffar, J. Kiwi, Langmuir 15 (1999) 185.
[7] R. Bauer, G. Waldner, H. Fallmann, S. Hager, M. Klare, T. Krutzler, S. Malato, P. Maletzky, Catal. Today 53 (1999) 131.
[8] X. Hu, F.L.Y. Lam, L.M. Cheung, K.F. Chan, X.S. Zhao, G.Q. Lu, Catal. Today 68 (2001) 29.
[9] J. He, W.H. Ma, J.J. He, J.C. Zhao, J.C. Yu, Appl. Catal. B 39 (2002) 211.
[10] J. Fernandez, J. Bandara, J. Kiwi, A. Lopez, P. Alberz, Chem. Commun. 14 (1998) 1493.
[11] Y. Zhang, M. Yang, X. Huang, Chemosphere 51 (2003) 945.
[12] Y. Zhang, M. Yang, X.M. Dou, H. He, D.S. Wang, Environ. Sci. Technol. 39 (2005) 7246.
[13] Y.B. Xie, C.W. Yuan, Appl. Catal. B: Environ. 46 (2003) 251.
[14] G. Wei, Y. Zhang, M. Yang, Y.X. Gao, L.P. Zhang, Tech. Equip. Environ. Pollut. Control 6 (2005) 7 (In Chinese, with English abstract).
[15] F. Martínez, G. Calleja, J.A. Melero, R. Molina, Appl. Catal. B: Environ. 60 (2005) 181.
[16] F. Wu, N.S. Deng, H.L. Hua, Chemosphere 41 (2000) 1233.
[17] R.M. Silverstein, G.C. Bassler, T.C. Morrill, Spectrophotometric Identification of Organic Compounds, 5th ed., John Wiley & Sons, Inc., New York, 1991.
[18] I.K. Konstantinou, T.A. Albanis, Appl. Catal. B: Environ. 49 (2004) 1.
[19] C. Hu, Y.Z. Wang, H.X. Tang, Appl. Catal. B: Environ. 35 (2001) 95.
[20] K. Tanaka, K. Padermpole, T. Hisanaga, Water Res. 34 (2000) 327.
[21] E.J. Weber, R.L. Adams, Environ. Sci. Technol. 29 (1995) 1163.
[22] C. Galindo, P. Jacques, A. Kalt, J. Photochem. Photobiol. A 130 (2000) 35.
[23] I.K. Konstantinou, T.A. Albanis, Appl. Catal. B: Environ. 42 (2003) 319.
[24] C. Guillard, H. Lachheb, A. Houas, M. Ksibi, E. Elaloui, J.M. Hermann, J. Photochem. Photobiol. 158 (2003) 27.
[25] J. Donlagic, J. Levec, Environ. Sci. Technol. 32 (1998) 1294.
[26] S. Nélieu, L. Kerhoas, J. Einthorn, Environ. Sci. Technol. 34 (2000) 430.
[27] C. Hu, J.C. Yu, Z.P. Hao, P.K. Wong, Appl. Catal. B: Environ. 42 (2003) 47.
[28] G.V. Buxton, C.L. Greenstock, W.P. Helman, A.B. Ross, J. Phys. Chem. 17 (1988) 513.